Comparative Analysis of Organic and Inorganic Solar Cells

Ricardo Raimundo
ricardo.raimundo@tecnico.ulisboa.pt

Instituto Superior Técnico, Lisboa, Portugal

November 2018

Abstract

The increasing need to make the planet more sustainable and the excessive use of finite resources in the production of energy makes the renewable resources crucial in order to satisfy the present energy demands without affecting natural resources and to ensure the survival of next generations.

The evolution of photovoltaic technology has been considerable and some new approaches try to improve their efficiencies, for example with use of other types of layers without compromised their cost.

Due to the limitation of the hours of sun, in a regular day, it is necessary to develop the photovoltaic technology and to improve their characteristics in order to occupy a prominent place in the renewable energies. In solar panels we can distinguish the ones which use organic semiconductor and the inorganic semiconductors. This study has the main focus on organic solar cells which produce the lowest impact in the ecologic environment when compared with traditional solar cells.

Several tests will be performed on organic solar cells in order to understand their advantages and disadvantages when compared with the silicon cells.

Keywords: Photovoltaic, renewable energy, sustainable, semiconductors, organic solar cells

1. Introduction

The increase of consumption of fossil fuels in the last century led to a natural resource depletion and introduced a ecologic footprint in our planet. The manifestation of negative effects generated by the fossil fuels, some of them almost irreparable, made the development of new alternative sources essential.

Alexandre Edmond Becquerel, in 1839, views the sun as a stable source of energy apposed to the wind or the sea, which are renewable sources of energy but are very unpredictable. To take advantage of the sun's energy, Alexandre tried to use that radiation in a experimental study. This let him to the discover of the photovoltaic effect and it was the first step to create, in 1877, the first device of conversion of photovoltaic energy.

There are three generations of solar cells. The first has the better efficiency/price relation and the most common semiconductor is the silicon, which can be mono-crystalline or poly-crystalline. The second generation of solar cells are the thin-films, composed by CdTe, a-Si or CIGS deposited on plastic or glass. The major disadvantage of these solar cells is the small conversion efficiencies. The third generation is made of organic and inorganic elements which are abundant in the nature such as PEDOT:PSS and silver. In this generation the easy recycling after its operation life is the most relevant feature.

The main objective of this study is to characterise and analyse organic solar cells and compare that with a photovoltaic thermal solar collector (CPVT), from Solarus AB. For this purpose several experimental test were made to understand not only the state of evolution of this technology as well as to draw a conclusion about the main advantages and disadvantages.

2. Literature review

2.1. Organic solar cells

The organic solar cells (OSC) are made of haled-based photosensitive organic materials. This materials have band-gaps in a range of 1.2eV and 3.5eV and are known as semiconductor or semiconductor conjugated due to their simple and double bounds. ITO (indium tin oxide) and FTO (flourine doped tin oxide) are usually used as oxide transparent semiconductors [7]. Typically a glass substrate is used to introduced a mechanical support and a anti-reflection to reduce the non-absorption losses.

The OSC can be divided in two categories, one of them that uses polymers is named Bulk heterojunction and other an the other one are based on small organic molecules is called the double-layer heterojunction [11]. The external functioning of the organic and inorganic cells is the same. The fact that organic cells do not have a crystalline constitution, such as silicon cells, will make it impossible for the same type of band-gaps just as an electric field will no longer be generated in the depletion zone in order to drive the electrons. The excitation caused by the photon is going to separated the carriers by the interface of the two material, in order to have more space for this effect is made the called bulk heterojunction which is a overlap of some thin layers between donor and acceptor material.

2.2. Organic semiconductors

The organic semiconductors could be classified in two categories, the small molecules and conjugated polymers. The small molecules have a molecular height of a few hundred of daltons (1 dalton= 1/12 Carbon), and not contain repeat unites as the polymers, which have a molecular height of 100000 daltons. The semiconductor made of small molecules have a weak solubility in the majority of the organic solvents and its preparation is made by vacuum thermal evaporation.

The polymers show a high decomposition and degradation when subjected to heat, this is due to the fact that their preparation is not made by thermal evaporation. Usually such materials are made by other methods such as spin coating, printing, spray coating or injected through other solutions making them extremely thin, flexible and inexpensive.

In the conjugated polymer cells there is a long chain of carbon atoms, so there is an enormous amount of very busy molecular orbitals (π - Higher Occupied Molecular Orbital) and of little occupied orbitals (π^* - Lower Unoccupied Molecular Orbital). The separation between LUMO and HOMO of a semiconductor is called a band-gap, and the electron affinity (E_a) corresponds to the lowest energy state of the conduction band (orbital π^*) and the ionisation potential (I_p) corresponds to the highest energy state of the valence band (orbital π) [7].

2.3. Types of geometries

2.3.1 Normal

In this geometry the ITO is coated in a way to smooth their surface and improve the potential in the anode. The coated layer must have properties that allow the transport of holes efficiently. The reinforcement of the potential in the anode helps to generate the electric field and improve the cell performance. On the top of ITO is deposited a hole transport layer which is made of several compounds as $MoO_3 - PEDOT : PSS$ that improve the stability of the cell. The active layer is laid on the hole transport layer and coated with LiF ou $CsCO_3$ immediately before the cathode [7].

2.3.2 Inverted

The inverted geometry solar cells are build in the same way of the normal geometry cells but with the carriers flowing the opposite direction. The ITO is used to receive the electrons through the cathode. To be efficient it must have a reduced potential and a higher band-gap. The potential between the two electrodes will allow the a development of the electric field which will drive the photo generation in the direction of ITO and the holes in the direction of the top electrode [7].

2.3.3 Single-layer heterojuction

In a single layer OSC only one layer is used to absorb the light between the two electrodes. Each photon is absorbed and generates an electron-hole pair, being necessary an specific amount of energy to separate them in a electron and a hole. For that purpose the electron-hole pair must diffuse through the interface of the cathode in a way to transfer the electron. The holes are left in the HOMO region and are transport them through the anode [7].

2.3.4 Double-layer heterojuction

The double-layer heterojunction has a structure where the donor and acceptor are laid one the top of each other to form a heterogeneous interface. In 1986, Tang developed the concept of electron donor and acceptor. This technique improved the dissociation of the electron-hole pair as well as the efficiency of the conversion [13]. This structure has stimulated the interest in organic solar cell.

2.3.5 Bulk

This Bulk structure is a blend of donor and acceptor material, building several interfaces in their connections. The concept was firstly used in polymer solar cells, in 1995. The low entropy of this structure promotes the blend separation. If the layers separation length were in the same range of the diffusion length, the majority of the pairs will disassociate on the surface of donor-acceptor. After that, the electron will be transported to the acceptor phase in cathode and the holes will be transported to the donor in the anode [7].

When is compared the double-layer with the bulk heterojunction it can be seen that the bulk will reduce their thickness and the probability of the recombination of the charge, causing a raise of the short circuit current density (J_{sc}) [14]. This cells approach the efficiency records for organic solar cell [8].

2.3.6 Hybrid double-layer heterojunction

The hybrid double-layer consist in a BHJ layer between the homogeneous layer of acceptor and donor material. It will improve the capture of the photon and the transport of the photo generated charges to the respective electrodes. The thickness of the homogeneous layers is chosen so that it approaches the diffusion length of the electron-hole pairs.

2.3.7 P-i-N

In this structure, the p and n material have a big band-gap and the active layers are laid between them which will substitute the non contribute layers in the transport of the charge. The efficiency of these cells are the double of similar cell without doped layers [10]. For that reason, the active layer could be produced with a few variety of thickness with no short circuits.

2.3.8 Tandem

In order to improve the absorption of the light spectrum incident on an organic solar cell the series structures were created. This cells have several layers on top of each other to optimise the absorption of the photon. In this way, the range of light spectrum is improved which is absorbed without increasing the internal resistance of the cell.

3. Experimental study

The solar panel has 0,2556m^2, more precisely 1,065 m and 0,24 m of length and width. Itś a product from the InfinityPV enterprise as well as the six demonstrators panels with a similar material but with an electrical difference. The study will make a comparison between the organic solar panel and the mono-crystalline silicon panel (CPVT, from Solarus AB). The organic solar panel has an open voltage of $V_{OC} = 130V/m$, short circuit current of $I_{SC} = 60mA$ and 5,2Wp, in STC conditions.

3.1. Study of the organic solar panel subject to different types of irradiance and temperatures

For a better understanding of the operation of this technology was analysed the *I-U* 1 and *P-U* 2 curve. The results illustrate how the parallel and shunt resistance affects the system. Consequently, the light incident on the organic solar panel was placed in 3 different positions, each one more distanced from the centre of the organic panel (table 1). The source of light was composed by two halogen lamps of 400W.

The *I-U* curve 1 shows the decrease of short circuit current I_{SC} due to the decrease of temperature in the organic cells. The equation 1 shows this relation.

Position	A	B	C
d (m)	1,33	1,63	1,94

Table 1: Distances from the central axis of the lamps to the centre of the panel.

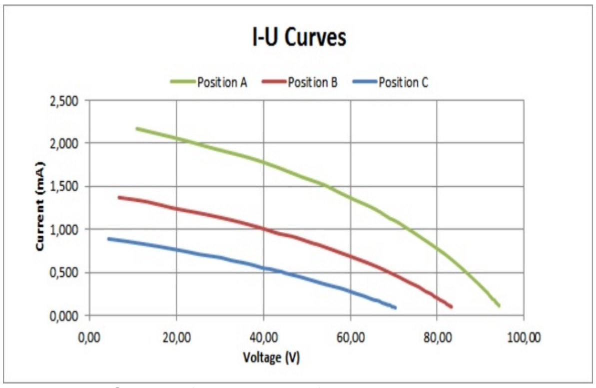

Figure 1: Graph of *I-U* curves for all positions tested in the laboratory.

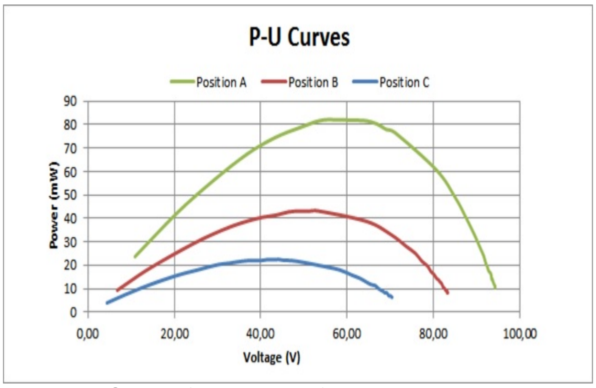

Figure 2: Graph of *P-U* curves for all positions tested in the laboratory.

The reduction of incident radiation on the surface of the panel occurs due to the displacement of the light source and consequently loss of energy, and also the open circuit voltage V_{OC} will be lower.

The ideality factor n and the saturation current I_{IS} are calculated from the diode equation 1. The results from the table 2 show a ideality factor between 6,156 and 6,257, quite high in comparison with a normal silicon cell (in the order of 2), is due to the chemical degradation of the cells after their manufacture.

$$I = I_S - I_D = I_{SC} - I_O(e^{\frac{V}{mV_T}} - 1)$$
$$V_T = \frac{KT}{q} \quad (1)$$

In order to prove how the short circuit current decreases with the increases of the temperature and how the open-circuit voltage increase with the incident radiation an experimental test was made. An almost transparent plastic was laid on the surface of the panel to create shading. Then the light

	n	$I_{IS}(\mu A)$	T (ºC)
A	6,247	172,6	29,6
B	6,659	175,6	27,9
C	6,156	141,3	27

Table 2: Table with non-ideality factor, inverse saturation current and panel temperature.

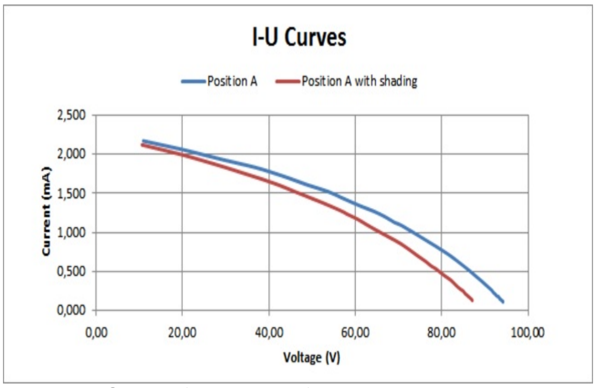

Figure 3: Graph of *I-U* curves for position A with and without shading.

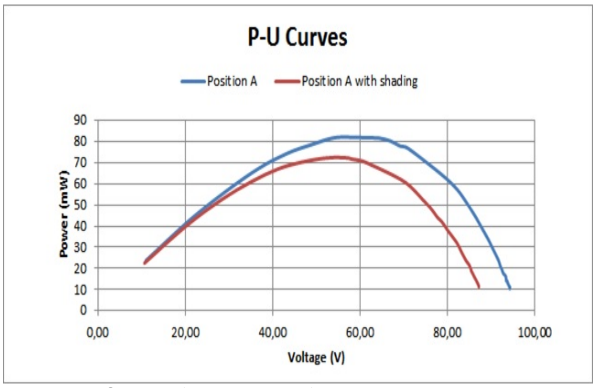

Figure 4: Graph of *P-U* curves for position A with and without shading.

source was placed on position A and the results of figures 3 and 4 were obtained.

3.2. Comparison between the silicon panel and the organic panel for the same distance from the light source

When comparing the normalised *I-U* curves 5 of the organic panel with the mono-crystalline panel it was found that in the organic panel there is almost linear growth as the charge is reduced. This behavior can be explained by the material type and the type of joints the panel is made of, which allows to absorb a greater number of wavelengths and give a higher current for lower voltage values. With this, the phenomenon of absorption of a larger number of photons, of higher wavelengths, allows the panel to obtain a *P-U* curve 6 with greater stability at its maximum operating point. The mono-crystalline silicon panel consists in two solar radiation absorption surfaces and a concentrator, one of which is located at the top of the panel and the

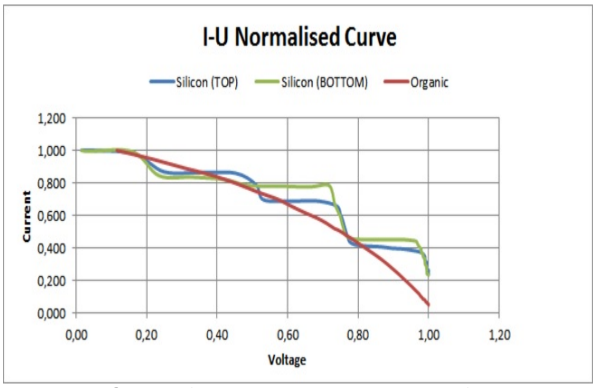

Figure 5: Graph of the *I-U* normalised curves for the silicon panel and for the organic panel.

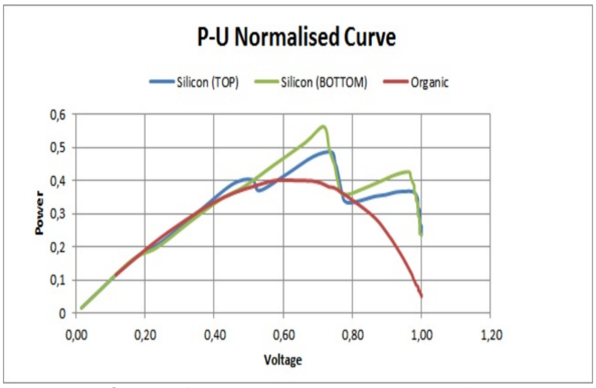

Figure 6: Graph of the *P-U* normalised curves for the silicon panel and for the organic panel

other at the Bottom.

3.3. Analysis of organic solar cells with different compounds

Organic solar cells can be composed of different organic structures. Thus, an experiment was carried out in which 6 different types of cells were used, specified with the following terms: A1, A2, A3, B1, B2, B3.

An analysis of the maximum operating point of each cell was made for a summer day, comprising periods of 2 hours and between 8 hours and 20 hours of that day. This experiment gave rise to the graph of the figure 7, thus allowing us to draw some conclusions about the relation between each cell.

In analyzing the figure 7, it is evident that there is a significant discrepancy of efficiencies between the set of cells A1, A2, A3 and B2 and the set B1 and B3. The first set has a range of efficiencies between 4,91-5,97%, with cell A1 having the best efficiency performance of the set of all cells. However, the set of cells with lower yields, between 1,48-1,66% at the maximum operating point, loses between 44,8-47,2% efficiency at the remaining hours of the day. The cell A3 is the one that has the best performances, with a maximum conversion efficiency of 5,1%, a maximum power of 344,6 mW, a power variation of about 52,3% and a variation of

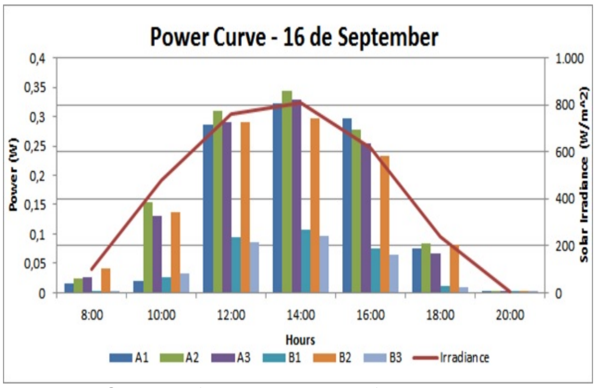

Figure 7: Graphic of the *P-U* curves of organic solar cells exposed to solar radiation.

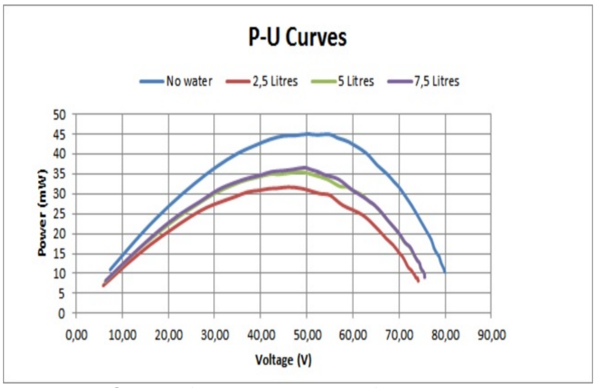

Figure 9: Graph of the *P-U* curves of the organic panel immersed in water.

conversion efficiency of 28,4%.

3.4. Simulate the immersion of the organic solar panel in water

The immersion of the organic panel was simulated in water, in order to observe the behaviour of the panel in a near real situation to understand the advantages of the application of this type of materials in aquatic environments.

The distance from the constant light source was kept at about 2,03m and the amount of water on the panel surface was varied. Four different experiments were done, one with transparent plastic (without water) and another three with 2,5 L, 5L and 7,5L of water inside the plastic, ilustrated in figure 8 and 9.

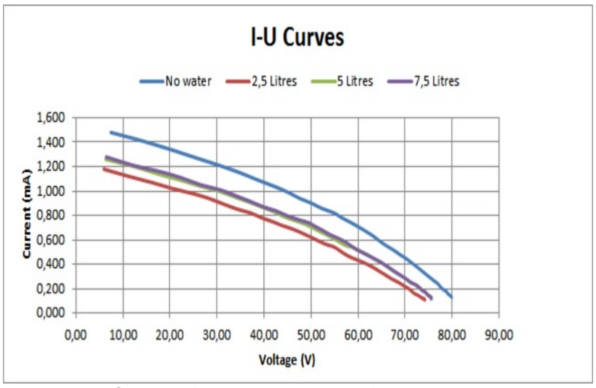

Figure 8: Graph of the *I-U* curves of the organic panel immersed in water.

In order to simulate the insertion of an organic panel into an aquatic environment, i.e. where the existing water is composed of organic matter and pollution, an experiment was conducted where the water on the surface of the panel is rendered turbid, allowing an approximation to the real situation.

Analysing the figures 8 and 9 it was possible to conclude that there was a decrease of the short-circuit current in the order of 11,75%, a decrease of the open-circuit voltage of 5,42%, and the maximum power point also decreased by about 18,24%. In this situation, the 7,5L turbid water power curve approached the 2,5L clean water power curve, which allow to conclude that by dyeing the water, the effect of radiation refraction on the panel was negated, improving the power curve with more than 5L of water and increase the reflection.

3.5. Organic solar panel subjected to different temperatures

In order to understand the potentialities of the organic solar panel for various types of installations an experiment was carried out. The panel was inserted inside a oven in the laboratory where the only aperture was to allow the passage of radiation from a filament lamp.

The oven was thermally insulated, thereby allowing the temperature inside to be varied. The temperature was varied from 10°C to 50°C, obtaining the characteristic curves of figures 10 and 11.

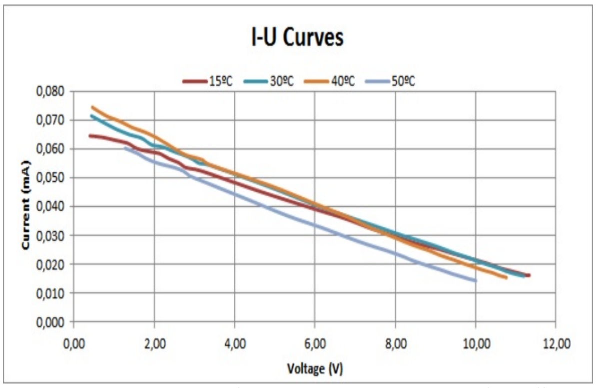

Figure 10: *I-U* curve of the organic solar panel for different temperatures.

From the results, it can be concluded that the V_{OC} decreases with increasing temperature, something that would already be expected in a mono-crystalline silicon cell and also occurs in this type of organic cells. However, the biggest difference observed is in the case where the temperature is increased from 40°C to 50°C. In this case

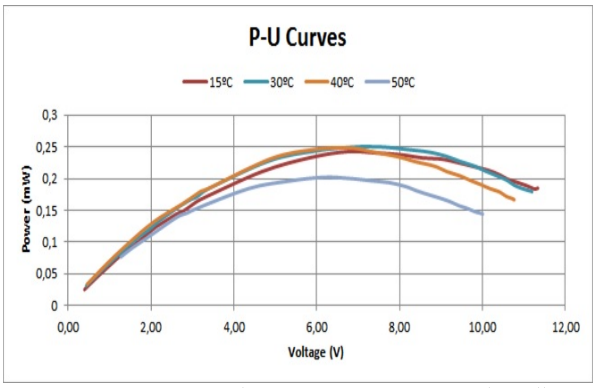

Figure 11: *P-U* curve of the organic solar panel for different temperatures.

there is a reduction of about 5% of the obtained power, however, this reduction can be very significant when the value of the powers involved are higher.

In order to realise how the non-ideality factor and the current I_{IS} were changed, the following mathematical expression were used:

$$I = I_{SC} - I_{IS}e^{\frac{U_D}{Xnv_T}} + I_{IS} \tag{2}$$

$$v_T = \frac{KT}{q} \tag{3}$$

deriving the equation 2, neglecting I_{IS} and choosing 2 points (A, B),

$$\frac{(I - I_{SC})_A}{(I - I_{SC})_B} = e^{\frac{U_{DA}-U_{DB}}{Xnv_T}} \tag{4}$$

$$n = \frac{U_{DA} - U_{DB}}{Xv_T \ln \frac{(I-I_{SC})_A}{(I-I_{SC})_B}}, \tag{5}$$

with X=224 (number of cells).
Then, the inverse saturation current I_{IS}, was calculated from the equation 2.

The results indicate that the non-ideality factor is between 1 and 2, so, despite the *I-U* curves do not have the normal geometry of a mono-crystalline silicon cell, the diode equation can approximate the equation that describes the operation of solar cells.

The evolution of the current I_{IS} grows as expected up to 40°C, hitherto the ratio between the increase of temperature and the increase of current I_{IS} is proportional. However, when the temperature rise above 40°C, the current I_{IS} begins to decrease progressively. The explanation for this phenomenon may be related to the introduction of dopants in these cells, which undergoes an action break from 40°C. The values obtained for the current I_{IS} correspond to an order of magnitude higher when compared to the mono-crystalline silicon cells and may indicate the lower concentration of dopants in the organic solar cells.

3.6. Operation of various types of sample solar cells under influence of IR radiation

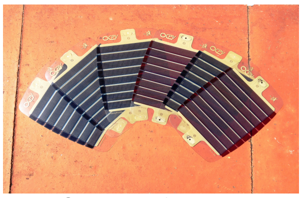

Figure 12: Samples of organic solar cells.

The manufacture of the organic cells does not follow a standard model and these can be improved by the introduction of dopants in their manufacturing process. In order to understand what influence these dopants may have on these cells, and how the absorbed radiation spectrum can reach the infrared range, six types of organic cells with different ratios of dopant material were analysed.

The cells used to do this experiment are the ones of the figure 12 and have six different denominations: A1, A2, A3, B1, B2, B3.

For this experiment a box with a single opening was used, where the IV filter is placed. For each cell a non-filter test and a filter test for the same solar irradiance were performed. The filter used corresponds to a band-pass of 1000/25 nm.

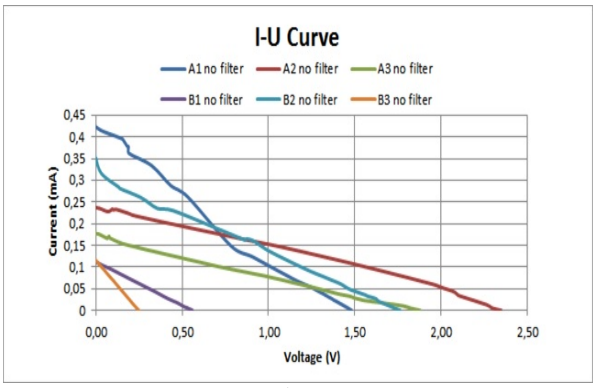

Figure 13: *I-U* curve of the various sample cells.

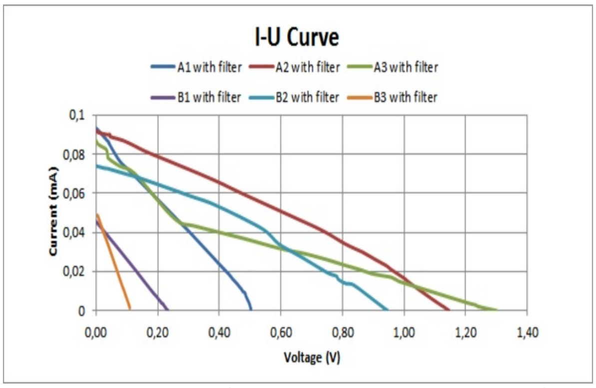

Figure 14: *I-U* curve of the various sample cells with IR filter.

Before analysing the results, it is important to know that the fill factor of an ideal cell can be given by the equation 6:

$$FF = \frac{V_{max} * I_{max}}{V_{OC} * I_{SC}} \quad (6)$$

Typically, the values for organic solar cells lie between 50-70% [9], although they fall below 25% when the *I-U* curve shown in figure 13 looks like a straight line. This is due to degradation of the cell and its organic components after minutes of its manufacture.

The cells used in this experiment were manufactured in Denmark a few months ago, as such, cell degradation had already started at the time of the experiments, having marked effects on its performance and the respective fill factor. Thus, the associated characteristic curves to the cells contain 25% fill factors, as can be seen in the figure 15.

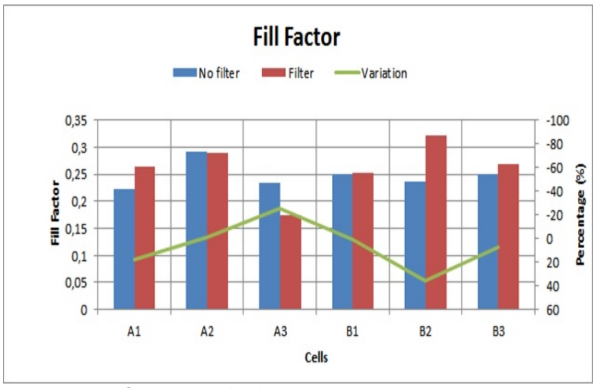

Figure 15: Graph the fill factor of the sample cells with and without the filter with the respective variation.

The reasons that caused cells to undergo this variation can be related to a reduction in charge extraction due to deterioration of the polymer/electrode interface, with the decrease in the mobility of the charge carriers over time and most probably due to the impurities of the materials, creating obstacles and leading to the reduction of its fill factor.

In general, the cells undergo an increase in the fill factor after insertion of the IR filter, this may be indicative of a reduction of the leakage currents in the contacts, derived from the reduction of the energy produced by the absorption of higher wavelengths.

3.7. Organic solar panel exposed to solar irradiance

The experiment carried out in this section aims to analyse how the OSC reacts in a situation where it is exposed to solar radiation. The panel being placed in the horizontal plane and directed towards the Sun. Measurements were performed every 2 hours in a time between 8 am and 8 pm, during 30 days not necessarily consecutive. The experiment was carried out in Lisbon, and apart from this experience a daily measurement was performed near Ourém.

By the analysis of the results illustrated in figure 16, it is verified that the power obtained for each hour are, on average, about 18 to 19 times higher than those obtained in the laboratory, (1-1,5 W on average per day). This can be explained by the fact that the solar spectrum covers a much longer wavelength range than a halogen lamp.

When analysing the characteristics of the two days for different location, the following was verified; (i) on July 31 (in Lisbon), an average power of 1.55 W per hour was achieved with an average incident radiation of 147.56 W per hour, (ii) on June 26 (in Ourém), an average power of 2 , 56 W per hour with an average incident radiation of 198.23 W per hour. Conversion efficiencies were 1.05 % for July 31 and 1.29 % for June 26, this shows that part of the energy emitted by the sun was being lost as solar radiation approached the land surface, in a more pronounced way in Lisbon than in Ourém, suggesting that the reason is associated with urban pollution.

The figure 16, represents the variation of the incident power and the power generated over the course of 30 days. This figure allows to visualise how the panel behaves with variations of solar irradiance. The large breaks on day 4 and day 8 are due to very cloudy periods, where the energy conversion was greatly reduced, and the average daily conversion efficiency's were 0,58% and 0,37%, respectively.

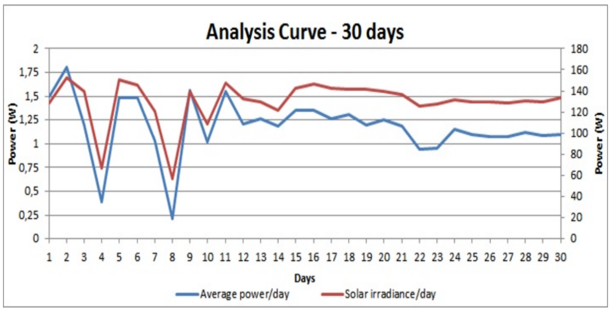

Figure 16: Daily average power curve over 30 days.

4. Comparative analysis

4.1. Economic analysis

Companies such as ASCA are in a development phase of OSC, but they can produce about 800 m/min of panel, reach about 1 million m^2 of OSC per year guaranteeing a lifetime of cells up to 20 years. Another company, Heliatek, provides a product with a lifetime up to 20 years, such as ASCA, and a payback time of less than 3 months. However, none of these companies made the purchase of an organic solar panel available on the website.

The mono-crystalline silicon solar panel, used for comparison, was chosen based on the maximum power produced at the maximum operating point.

$Type$	Mono-Si	Organic
$Model$	MM005-12/1	infinityPV foil
$P_{MP}(W)$	5	5,2
$\eta(\%)$	≈ 8.2	≈ 4
nº Cells	36	224
$Weight(kg)$	0,8	0,22-0,45
$Size(mm)$	180x340x23	1050x0,305
$Cost/unit$	14,5	175
$Cost/Wp$	2,9	33,65

Table 3: Electrical and mechanical characteristics of the two technologies.

From the technical characteristics of table 3, it is possible to conclude the relationship between the price per Watt of the organic panel and the mono-crystalline silicon panel. The acquisition cost of an organic power panel of 5,2 W acquired from InfinityPV is about 11,6 times more expensive. However, the applications of these technologies are different as well as the stage of their evolution.

4.2. Production Analysis

OSC, produced by InfinityPV, are manufactured using the R2R method, which consists of a manufacturing process using an industrial printer with a roll of plastic substrate to serve as a base for the cells compounds printing. The module layout is terminated by printing the rear silver electrodes to cover the PEDOT: PSS layer and make the connection to the front electrode bus. The prints are usually dried through hot air at 140ºC and using infra-red lamps [6].

The manufacturing processes of this type of cells allow the use of a semi-manual process, producing about 100m/min, and an automated process producing between 2-300m/min, so, in terms of speed the production of this technology is ready to compete in the renewable energy market.

The mono-crystalline silicon can be obtained by two methods, the Czochralski method (CZ) and the fusion zone method. The CZ method consists in a slow extraction of the silicon cylindrical crystal using a quartz crucible, containing molten poly-crystalline silicon and some dopant elements such as Boron and Phosphorus, in order to create a p or n layer, respectively. A silicon crystal seed is inserted into the liquid poly-crystalline silicon in a rotating manner and the quartz crucible begins to descend progressively, in an inert atmosphere (usually Argon). This process gives rise to a mono-crystalline silicon ingot, and the ingots may be between 200-300kg and may have lengths of 2m [12].

The entire production process of a mono-crystalline silicon wafer is quite expensive and time consuming. High temperatures are required to allow melt levels and purity of suitable materials to be achieved.

It can be concluded that the production process of an OSC is considerably less expensive at the energy level, not only because it is a much faster production but also because it is made at considerably lower temperatures, compared to production of silicon cells.

4.3. Degradation Analysis

OSC may be subject to small holes and scratches at the time of installation, and the impact of small and large poultry waste. The panel may allow water and oxygen penetration during the hours of operation, causing damage to the intermediate layers, the degradation of the active layer, the dissolution of PEDOT: PSS and oxidation of the electrodes of silver.

In order to find hot spots on the organic panels, infrared imaging techniques are used. The current begins to accumulate in a zone of low resistance, heating that zone of the cell and giving rise to a burn.

The junction zone of the electrodes on the side edge of the panel is also susceptible to creating small burns due to delamination and subsequent inflow of water around the edges.

Atmospheric phenomena, such as storms and lightning followed by heavy rainfall cause serious damage to the panels, since they can not be switched off during operation.

The UV radiation and the water, combined with temperatures above 50ºC, give rise to a chemical alteration of the EVA (adhesive material between glass and cells), causing a change in light transmittance and consequent reduction of the overall power. The visible reaction of this effect is given by the appearance of a yellowish or brownish hue at the junction between the cells.

The loss of adhesion between the different layers of the modules causes an increase in reflection of the light beams and penetration of water within the panel. In the worst case, the loss of adhesion at the edges of the module and so, the electrical risk of the panel and of the whole installation is high, as well as the corrosion of the metals.

The appear of bubbles is caused by an adhesion failure between the panel and the EVA, caused by a chemical reaction and where some gases are released. The less heat dissipation on the cell provokes a overheating and a lifetime reducing. Normally, bubbles appear in the centre of cells and in some situations they are only identified with optical techniques using infrared radiation.

Given the attempt to reduce production costs, the manufacture of silicon cells has been reducing its size. This has a direct relation with the increase in the fragility and susceptibility of the cells, giving rise to possible fractures during the manipulation, lamination and storage. Micro-fractures have a very large influence on both cells consistency and the possible reduction of the path of recombination of the charge.

Finally, the appearance of hot spots may be a consequence of different situations, such as partial shading, cell incompatibility or cell-to-cell faults. To avoid the reversed operation of the shaded cells, by-pass diodes are used. However, diodes are not always adequate, leading to excessive heating and causing irreversible cell damage.

Although it is not possible to predict the occurrence of defects in both technologies, it is possible to infer that when a replacement of a part of an organic panel occurs, its repair will replace it partially. When replacing a damaged cell in a silicon panel it is necessary to replace the entire panel. This analysis makes clear that it is preferable that a defect occurs on an organic panel.

4.4. Applicability of OSC

In 2012, it was developed in Frankfurt, by the company Opvius, the first OPV installation connected to the grid. It had a capacity of about 0,2 kW and the objective was to study its static and mechanical capacities during the generation of energy. After 4 years of operation, the system demonstrated a good behaviour [2].

The same company developed in 2015, in a cover of the African Union Building, in Addis Ababa, Ethiopia, an OPV system with about 1800 semi-transparent cells, in 450 modules and occupying around 500 m^2, allowing to feed the LED light system of the building [1].

Heliatek, a company that works in the R&D and marketing of OSC, has installed a system of electric energy production at a Biogas plant in Berghein-Paffendorf, Germany, combining 2 green energies. The installation has a capacity of 5,4 kWp and was installed vertically in the steel profile of the plant, without the need for ventilation or considerable mechanical support. This was only possible given the flexibility and lightness of this technology [3].

In 2017, Heliatek developed another pilot project, creating the largest BIOPV facility in the city of La Rochelle, France, with a production capacity of 22,5 kWp and occupying about 500 m^2, each panel strip having 2, 4 and 5,7 m. The system was installed by 6 people and took about 8 hours to be complete [4].

Opvius refer to the automotive market, which in particular has a case study, OSC were inserted in the wind deflector of a truck, in order to limit the discharges in the batteries of the vehicle, thus increasing its life time [5].

The company Heliatek is in a phase of testing the development of car roofs to provide ventilation (while the car is parked), improve air-conditioning performance and reduce battery power loss peaks, increasing their useful life.

4.5. Advantages and disadvantages

The major advantages of mono-crystalline silicon solar cells are the cost of acquisition, given the current mass production, the energy conversion capacity, which is much higher than that of OSC, and all the studies already done on this technology. However, organic solar cells are being studied more and more intensively, thanks to their unique characteristics. This may mean that in a few years we will see a massification of this technology, leading to a reduction in the price per Watt for the final customer.

5. Conclusions

The search for ecologically sustainable electronic components and with an active role in energy generation has brought the possibility of discovering new manufacturing methods, new materials and a new way of looking at all the potentialities that nature offers us.

The present study was based on OSC, taking into account the fact that they are associated with an emerging manufacturing technology with great potential, with a strong ecological component and with a large mass production capacity.

The study carried out has an experimental component and numerical simulation taking into account the information provided by the manufacturers or the ones associated to data collection on climate and radiation from meteorological stations.

For the case of monocrystalline silicon cells, the stationary power-voltage characteristics present several relative maximums in the presence of shadings associated with adverse radiation conditions. The same does not happen with OSC that have *P(U)* characteristics with only a maximum. The diversity of power peaks, in the case of silicon cells, makes the search for the Maximum Power Point Tracking (MPPT) harder: either in the numerical simulation tools in a theoretical analysis or in the mechanical tracking control processes in non-stationary solar panels.

Through the simulation of immersion of the panel in water, the studies carried out concluded that the organic panel is very sensitive to changes in temperature, improving its performance as the temperature of the cell decreases, with the introduction of cooler liquid medium. The results show that the ideal operating temperature of the organic solar cells is between 15-40ºC, obtaining a power loss of 0,5% for each degree Celsius above 40ºC.

Another factor that influences the performance of the panel is related to the refractive capacity of the liquid, obtaining the best results for a depth of 0.64cm of water.

By simulating the operation in a near real environment with the insertion of suspended particles in water, there was a decrease in energy efficiency of approximately 18%, at the Maximum Power Point (MPP).

The analysis of OSC samples had also led to the conclusion that there are several possible combinations of organic elements in quantitative terms, in a situation very similar to the one created by Boron and Phosphorus doping the p and n layers of monocrystalline silicon solar cells.

In order to analyse the behaviour of the organic panel, at the maximum operating point, when exposed to solar radiation, seven measurements were performed per day (from eight a.m. to eight p.m.) for 31 days. Qualitatively, the results obtained were as expected, although quantitatively the results obtained for the peak power values were slightly below the 5 W, according to the data provided by the manufacturer, suggesting real conditions very different from the test.

Regarding to manufacturing technology, it can be concluded that Roll-to-Roll technology represents a very adequate and effective method, taking into account the versatility, speed and quality of reproduction of organic panels. However, more projects will be needed to effectively demonstrate all the potential of this technology. It may, however, be pointed out that OSC require less energy-intensive and more innovative technologies. Organic solar cells are still at an embryonic stage of development and commercialisation.

References

[1] Grid-connected opv system, mainova ag in frankfurt, germany. http://www.opvius.com/grid-connected-opv-system.html, 2012.

[2] Opv sail in shape of african continent, african union peace and security building in addis ababa. http://www.opvius.com/energy-generating-shade-sail-in-shape-of-african-continent.html, 2015.

[3] First time installation of organic solar film on biogas plant with innogy. https://www.heliatek.com/en/applications/pilot-projects, 2016.

[4] Worlds largest biopv installation with heliasol in la rochelle, france. https://www.heliatek.com/en/applications/pilot-projects, 2017.

[5] Opv enforced wind deflector for truck, jmk logistik gmbh, germany. http://www.opvius.com/opv-wind-deflector-for-trucks-288.html, 2018.

[6] M. Hösel, R. R. Sondergaard, M. Jorgensen, and F. C. Krebs. Fast inline roll-to-roll printing for indium-tin-oxide-free polymer solar cells using automatic registration. *Energy Technology*, 1(5):102–107, 2013. DOI: 10.1002/ente.201200029.

[7] P. Kumar. *Organic Solar Cells: Device Physics, Processing, Degradation, and Prevention*. CRC Press Taylor and Francis Group, 2017. ISBN:978-1-4987-2327-5.

[8] Y. Liu, J. Zhao, Z. Li, C. Mu, W. Ma, H. Hu, K. Jiang, H. Lin, H. Ade, and H. Yan. Aggregation and morphology control enables multiple cases of hingh-efficiency polymer solar cells. *Nature Communications*, Nov 2014. DOI: 10.1038/ncomms6293.

[9] B. Qi and J. Wang. Fill factor in organic solar cells. *Physical Chemistry Chemical Physics*, 15(23):8972, Apr 2013. Doi:10.1039/C3CP51383A.

[10] J. Rostalski and D. Meissner. Monochromatic versus solar efficiencies of organic solar cells. *Solar Energy Materials and Solar Cells*, 61(8):87–95, 2000. DOI:10.1016/S0927-0248(99)00099-9.

[11] V. Shrotriya, G. li, Y. Yao, T. Moriarty, K. Emery, and Y. Yang. Accurate measurement and characterisation of organic solar cells. *Advanced Functional Materials*, 16(7):2016–2023, Oct. 2006. DOI:10.1002/adfm.200600489.

[12] P. Siffert and E. F. Krimmel. *Silicon Evolution and Future of a Technology*. Springer, 2^{nd} edition, 2003. ISBN: 978-3-642-07356-4.

[13] C. W. Tang. Two-layer organic photovoltaic cell. *America Institute of Physics*, 48(183), 1986. DOI: 10.1063/1.96937.

[14] J. Xue, B. P. Rand, S. Uchida, and S. R. Forrest. A hybrid planar-mixed molecular heterojuncion photovoltaic cell. *Advanced Materials*, 17(5):66–71, 2005. DOI:10.1002/adma.200400617.